

# EXPERIMENTALLY VALIDATED STUDIES OF THERMOELECTRIC GENERATORS INSTALLED ON A COMPRESSOR TEST BENCH

CLAUDIA SĂVESCU<sup>1</sup>, ALEXANDRU M. MOREGA<sup>2</sup>, MIHAELA ROMAN<sup>1,2</sup>, CRISTIAN NECHIFOR<sup>1,\*</sup>

**Keywords:** Thermoelectric generators; Waste heat; Energy harvesting; Industrial compressor; Finite element analysis (FEA).

This paper presents preliminary experimental work on a twin-screw compressor, aiming to validate numerical studies and demonstrate the potential of thermoelectric energy harvesting. Considering two thermoelectric modules, the experimental validations are conducted in an industrially relevant environment on a test bench for industrial air and gas compressors. The digital twin was simulated using finite element analysis, provided with a heat sink, and a fully coupled heat transfer and electric field was solved to assess the thermoelectric effect. This allows for complete modeling of the Peltier-Seebeck-Thomson effects. The compressor vibrations are also introduced for structural analysis to ascertain that the bismuth telluride thermoelectric modules are safe to use under sinusoidal mechanical vibrations. The thermoelectric generators are screwed onto the hottest part of the compressor skid, specifically the multiplier gearbox cover, which is splashed with hot lubrication oil from within. After the thermal stabilization of the compressor, we obtained a constant series voltage of around 0.4 VDC from the two thermoelectric generators, and the series current was measured to a value of 115 mA.

## 1. INTRODUCTION

Any industrial process and machine that produces mechanical work [1–5] inherently produces waste heat as a by-product, often dissipating into the atmosphere. The waste heat can also limit a machine's efficiency and cause thermal aging.

Thermoelectric generators (TEGs), a non-conventional micro-energy harvesting source, have been researched more thoroughly over the last two decades, along with the rapidly expanding technologies for energy harvesting [6–10] and renewable energy [11–16]. Solid-state TEGs are reliable solutions to exploiting and harnessing waste heat [17]. They can harvest energy by converting heat into electric energy, driven by temperature differences (or gradients), and their principle of operation relies on the Seebeck effect.

Most research articles on thermoelectric generators take a theoretical approach. Most deal with only one thermocouple, not an entire thermoelectric module with several n-p semiconductor pairs coupled electrically and thermally [18]. Additionally, the analyses are conducted over relatively arbitrary temperature ranges to maximize electric power [19–23].

The maximum power output specified for the TEGpro 10 W thermoelectric modules employed herein, TE-MOD-10W4V-40 [24], corresponds to a temperature difference of more than 200 °C, which is impossible to achieve in our practical application involving a twin-screw compressor and would be difficult to maintain even in laboratory conditions. Ensuring forced convection cooling of the cold side would be ideal; however, this implies the use of fans or water pumps, which renders the very purpose of micro energy harvesting void, as powering these devices would consume more power than the TEGs can generate.

The paper presents preliminary experimental work carried out on an industrial compressor test bench. The digital twin model simulated using the finite element analysis (FEA) [25] concerns a heatsink and considers the temperature ranges previously measured on the compressor. Thus, we could conduct a proper experimental validation of the numerical simulation results.

The experimental test presented relies on previous works involving numerical simulations and analytical models [26–28], as well as a series of studies assessing the compressor's

vibrations and thermal footprint [28,29]. TEGs are part of a multisource energy harvesting system together with piezoelectric harvesters [30]. The present study, focusing on the thermoelectric aspect, takes a step forward towards *in-situ* applications by adopting a practical approach, implementing thermoelectric devices on an industrial twin-screw compressor test bench (Fig. 1). A technology readiness level (TRL) of 6 is achieved, demonstrating the technology in an industrially relevant environment.

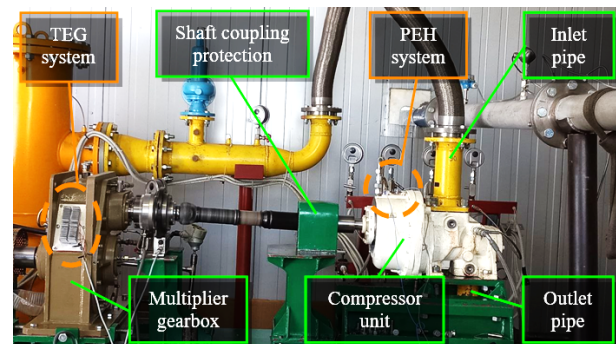


Fig. 1 – Compressor skid, at the headquarters of the Romanian Research and Development Institute for Gas Turbines COMOTI [31].

## 2. THERMOELECTRIC SIMULATIONS

Figure 2 presents the TEGpro TE-MOD-10W4V-40 thermoelectric module. Three such modules have been acquired, two of which are employed herein. Their overall dimensions are 40 mm × 40 mm × 5 mm (L × W × H). The manufacturer claims that these can provide an output power of up to 10 W and a voltage output of 4 VDC [24] for a temperature difference of ~200 °C.

The temperature ranges introduced in finite element simulations follow the temperatures recorded on the housing of the housing of the twin-screw compressor. A gas exhaust temperature limit is set within the automation control software, an automatic shutdown sequence being performed when this threshold is reached, normally around 75-80 °C, depending on the lubrication oil injected, since higher temperatures may cause a faster thermal aging and deterioration of the lube oil.

Since higher hot side temperatures may be unattainable for

<sup>1</sup> Romanian Research and Development Institute for Gas Turbines COMOTI, Bucharest, Romania.

<sup>2</sup> National University of Science and Technology Politehnica Bucharest, Romania. E-mail: alexandru.morega@upb.ro.  
E-mails: claudia.borzea@comoti.ro; alexandru.morega@upb.ro; mihaela.roman@comoti.ro; cristian.nechifor@comoti.ro (corresponding author).

the TEGs, cooling the cold side would be beneficial for providing a higher temperature gradient across the module, which is desirable for increasing the electric output. Proper ventilation of the cold side should be provided as well.

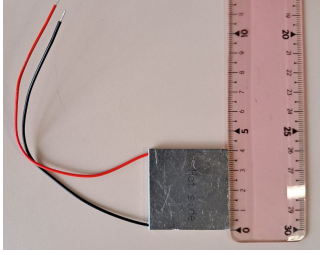


Fig. 2 – Thermoelectric generator TEGpro TE-MOD-10W4V-40.

For the numerical model's computational domain, 72 thermocouples were used, relying on the insight into the inner construction for three commercial thermoelectric modules provided in [32], and observing the number and arrangement of the thermocouple arrays. The geometry of the numerical model in Fig. 3 was designed relying on a parametrized application builder [33], intended for thermoelectric coolers, but easing the model building for thermoelectric modules geometries regardless of application.

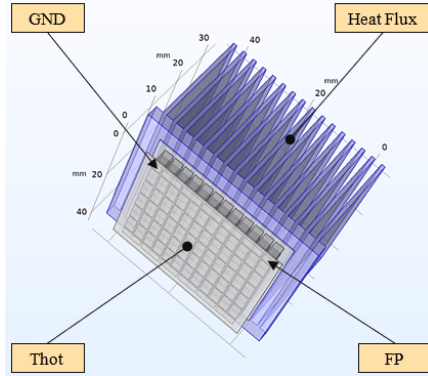


Fig. 3 – Digital twin with heatsink and declared boundary conditions.

The material properties used in the simulation program are presented in the Appendix (Table 2). The manufacturer does not disclose information on  $\text{Bi}_2\text{Te}_3$  properties used for the modules. The  $n$ -type and  $p$ -type  $\text{Bi}_2\text{Te}_3$  are assumed to have same values [33].

The numerical simulations unveil the coupling of heat transfer and electric field [18] for the full modelling of Peltier-Seebeck effects and for the resistive heating (Joule effect). They involve interconnecting two physical models with an electrical circuit model, which simulates the electric load, in a hybrid field-circuit ensemble. The TEG powers a resistive load,  $R$ , which is used to evaluate the efficacy of energy harvesting when the TEG is associated with the compressor.

The physics and mathematical model concern:

- The heat transfer problem:

$$\begin{aligned} \nabla \cdot \mathbf{q} + \dot{Q} &= 0, \\ \mathbf{q} &= -k\nabla T, \end{aligned} \quad (1)$$

where:  $\rho$  [ $\text{kg}/\text{m}^3$ ] – density;  $T$  [K] – temperature;  $\mathbf{q}$  [ $\text{W}/\text{m}^2$ ] – conduction heat flux;  $\dot{Q}$  [ $\text{W}/\text{m}^3$ ] – heat (Joule power) source; and  $k$  [ $\text{W}/(\text{m}\cdot\text{K})$ ] – thermal conductivity.

- The electric field problem:

$$\nabla \cdot \mathbf{J} = 0,$$

$$\mathbf{J} = \sigma \mathbf{E} + \mathbf{J}_e, \quad (2)$$

$$\mathbf{E} = -\nabla V,$$

where:  $\mathbf{J}$  [ $\text{A}/\text{m}^2$ ] – conduction electric current density;  $\sigma$  [ $\text{S}/\text{m}$ ] – electrical conductivity;  $\mathbf{E}$  [ $\text{V}/\text{m}$ ] – electric field;  $\mathbf{J}_e$  [ $\text{A}/\text{m}^2$ ] – a source term that accounts for the thermoelectric effects; and  $V$  [V] – electric potential.

- The thermoelectric effects are introduced through:

$$\mathbf{q} = \alpha T \mathbf{J}, \quad \mathbf{J}_e = -\sigma \alpha \nabla T, \quad (3)$$

where:  $\alpha$  [ $\text{V}/\text{K}$ ] – Seebeck coefficient.

The boundary conditions that close the model are as follows:

- For heat transfer: an initial hot side temperature,  $Thot$ ,  $100^\circ\text{C}$  is set, and a convective heat flux (external natural convection with air at 1 atm,  $20^\circ\text{C}$ ) is declared instead of  $Tcold$  used in previous works [26, 28]. For this model, also provided with a heatsink, a thermal contact condition is added on TEG's cold side boundary.
- For the electric currents: ground (GND) and a floating potential (FP) condition type Circuit are declared on the faces of the terminal legs.
- For the external electrical circuit, the node connections are ground and floating potential, derived from the electric currents interface, for a resistor ( $2.4\text{ k}\Omega$ ) load.

## 2.1 STATIONARY STUDY

A stationary study with a parametric sweep of the hot side temperature,  $Thot$ , range( $30,5,100$ )  $^\circ\text{C}$ , was conducted. The computed power [25] is relative to resistive load. The voltage, current and power are plotted on the graph in Fig. 4.

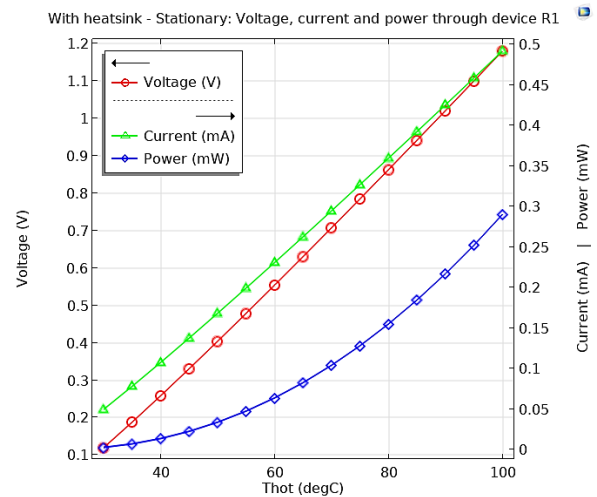


Fig. 4 – Stationary study: voltage, current and power.

An improvement of about one order of magnitude, in natural convection conditions, is achieved when using the heatsink, compared to the results obtained without [27]. The maximum electrical parameters, obtained with heatsink at  $Thot = 100^\circ\text{C}$ , are 1.2 V,  $\sim 0.5$  mA, *i.e.*,  $\sim 0.3$  mW.

## 2.2 TIME DEPENDENT STUDY

It is worthwhile to see how the thermoelectric generator's output behaves over time, and how fast this one stabilizes thermally. A time dependent study, range( $0,1,60$ ) min was run to observe the thermal stabilization between hot and cold sides, taking  $Thot = 100^\circ\text{C}$ . The initial conditions considered

are a temperature of 20 °C and null electric potential.

The physics that describes the TEG time dependent working conditions are as follows:

- Heat transfer:

$$\rho C_p \frac{\partial T}{\partial t} + \nabla \cdot \mathbf{q} = \dot{Q}, \quad (4)$$

$$\mathbf{q} = -k \nabla T.$$

- Electric field: the significant difference between the heat transfer and electric field time scales recommends using an electrokinetic model.

$$\nabla \cdot (-\sigma \nabla V + \mathbf{J}_e) = 0. \quad (5)$$

- The thermoelectric couplings are described by eq. (3).

The graphs in Fig. 5 shows that the simulation program reliably provides the results after the thermal stabilization program of the TEG. Additionally, the time dependent study offers extra information about the heatsink effect on the electrical parameters, these ones decreasing more smoothly and maintaining values with almost one order of magnitude higher than without heatsink [27]. The stabilization values are the same as specified in the stationary study above.

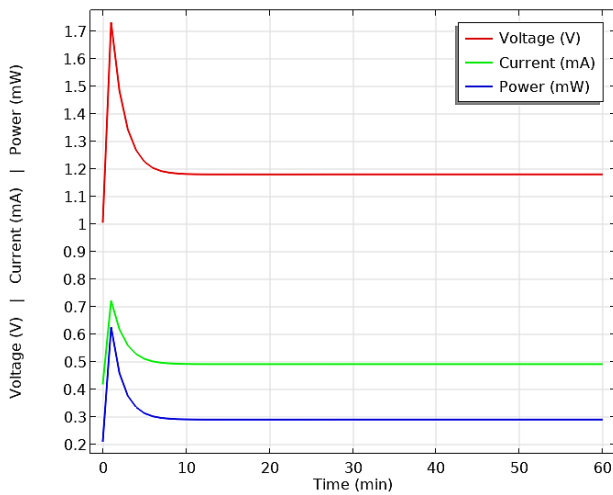


Fig. 5 – Time Dependent study – voltage, current and power.

### 2.3 FREQUENCY DOMAIN STUDY

For a proper numerical assessment matching the experimental conditions, Solid Mechanics physics interface was also introduced to account for compressor vibration amplitudes measured on the compressor at the rotational speed of 2500 rpm [29].

For the structural study, a prescribed velocity was applied on the exterior hot side boundary, in all directions, as follows:  $v_x = 0.998$  mm/s,  $v_y = 2.985$  mm/s,  $v_z = 1.692$  mm/s. Filling in Young's modulus ( $E = 32$  GPa) and Poisson's ratio ( $\nu = 0.25$ ) for Bismuth Telluride was required [34].

Figure 6 shows a peak von Mises stress value of 14.1 kPa. This value is negligible compared to the yield strength of the  $\text{Bi}_2\text{Te}_3$  thermoelectric material used, which can withstand compression stress values of up to 62 MPa, according to [34].

After running this structural analysis, we can conclude that the vibrational behavior of the rotary screw compressor does not present any risk whatsoever to damage the thermoelectric modules placed on the compressor skid, even with the highest vibration amplitudes measured on the compressor unit introduced in the simulation. The gearbox vibration levels are much lower and will be measured within upcoming

experimental research works.

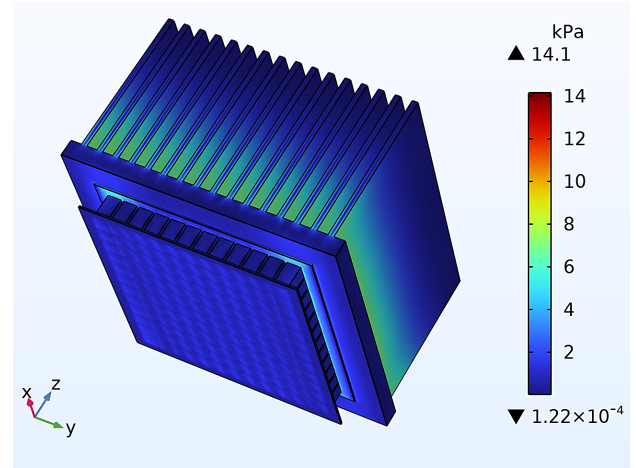


Fig. 6 – Von Mises stress evaluation for 83.5 Hz.

### 3. EXPERIMENTAL SETUP

Before attempting the installation, certain guidelines should be followed to ensure the proper mounting of thermoelectric generator modules, to prevent damages and for increasing the conversion efficiency. Because of the materials' thermal expansion that occurs during normal operation at large temperature differences, it is strongly recommended to use special hardware for avoiding the module's damage. For a proper mounting, even pressure must be applied on both sides of the module [35].

Thermal conductive paste was applied on both sides. The heatsinks were screw mounted onto the duplicate gearbox cover. A torque per screw of 1.25 Nm (0.128 kg·m) is recommended by manufacturer [35]. A torque screwdriver within the required range was used for the purpose.

The TEG system was installed on the duplicate gearbox cover (Fig. 7). The replacement cover, together with the thermoelectric harvesting system, were then installed onto the gearbox.

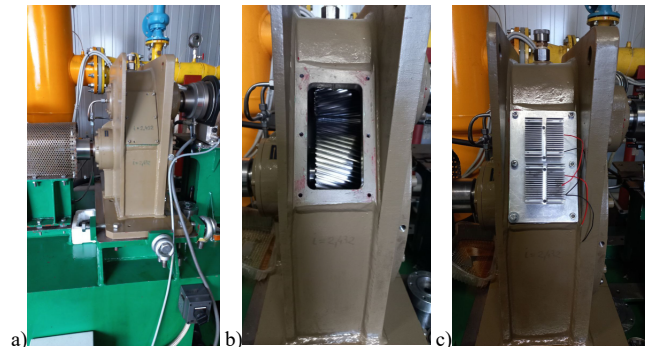


Fig. 7 – a) Multiplier gearbox with original cover, b) Cover removed and view of the gears; c) TEGs installed on duplicate cover.

Even though the tests do not necessarily require having a compressor on the test bench, the gearbox oil heats more if the compressor is provided as load in the kinematic chain, due to more mechanical work being produced, which is preferred for the application proposed. The gearbox cover is splashed with hot lubrication oil from the underneath.

The thermographic image in Fig. 8 was taken during the experimental tests, proving that the hottest mounting spots chosen for the TEGs were chosen very well after the compressor's preliminary thermal scans.



The graph below shows the separate voltage outputs rendered by the two thermoelectric modules. As expected from the thermal analysis above, although they start from approximately the same voltage outputs, TEG2 reaches a higher maximum voltage than TEG1 after the compressor has stabilized thermally. The data in Fig. 14 were recorded over almost one hour (48 minutes), between 11:22 and 12:10.

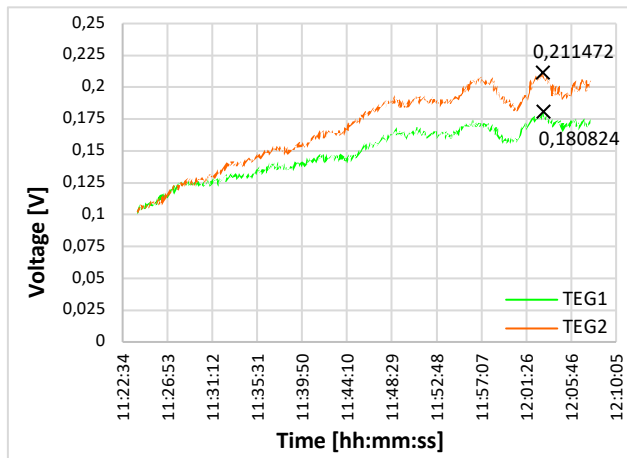


Fig. 14 – TEG1 and TEG2 voltage outputs.

The two modules were connected in series, resulting in a summed voltage output. The series connection was established after separate measurements, when the compressor had already reached thermal stability and no further temperature increase occurred. A constant series voltage between approximately 0.377 VDC and 0.414 VDC was recorded from 12:12:32 to 12:14:54 (Fig. 15). The series current was measured with the multimeter at 115 mA (Fig. 16).

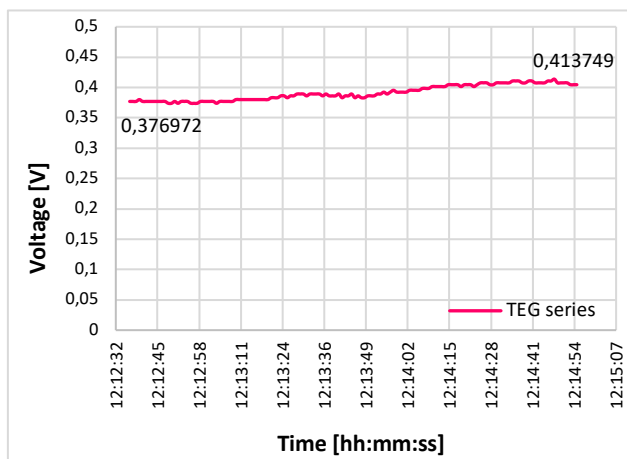


Fig. 15 – Series voltage output of the two thermoelectric generators.



Fig. 16 – Thermoelectric series current.

Thermoelectric generators are easy to install and exhibit stable electric output. They also have the advantage of output in direct current for powering low-consumption devices. This gives thermoelectric generators a higher robustness than the piezoelectric part of the multisource energy harvesting system envisaged, and their output consistency confers standalone potential.

The electrical parameters obtained experimentally for the series connection are summarized in Table 1.

Table 1  
Experimental thermoelectric output parameters

No.	Quantity	Series value	Unit
1.	Maximum voltage	0.414	VDC
2.	Maximum current	115	mA
3.	Maximum RMS power	47.61	mW
5.	Temperature gradient (average)	3.5	°C

## 5. CONCLUSIONS

The paper presents the digital twin simulation model and experiential works conducted on an industrial compressor test bench. The boundary conditions considered in the finite element simulations are realistic data measured on the compressor, and the digital twin model is built according to the physical TEGs.

This research aimed to assess the effects of electrical parameters that we can realistically expect from harvesting industrial waste heat rather than obtaining as high values as possible for the thermoelectric power. Using a multisource approach, the thermoelectric generators may also be a backup source for piezoelectric vibration harvesting.

The frequency domain study showed that the compressor's triaxial sinusoidal mechanical vibrations do not pose a threat to the thermoelectric modules. This analysis was critical to conduct before the experiments. The stationary study showed pertinent results comparable to the plots in the product specifications. The curves obtained for current, voltage, and power validate the correctness of the model.

The numerical analyses show that adding a heatsink improves the thermoelectric power output, even in natural convection conditions. Future research will focus on enhancing thermoelectric production through externally forced convection. The heatsinks shall be rotated at 90°, as the lateral walls of the gearbox prevent air circulation. Additionally, the time-dependent indication shall be conducted when a auxiliary sweep of *Thot* is performed.

The differences between the simulations and the experiment may be due to the limited data provided by the manufacturer and the varying electrical loads. Proper experimental measurements acquiring the current in time shall be pursued, along with matching numerical simulations considering the measurement devices' impedances, as well as with the components of an energy harvesting circuitry.

## ACKNOWLEDGEMENT

The numerical simulations were conducted at the Faculty of Electrical Engineering, from the National University of Science and Technology Politehnica Bucharest.

The first, third, and fourth authors acknowledge the work realized as part of "Nucleu" Program within the Romanian Research, Development and Innovation Plan 2022-2027, conducted with the support of the Romanian Ministry of Research, Innovation and Digitalization, as part of contract 31N/2023, project number PN 23.12.09.01.

## APPENDIX

Table 2

Thermoelectric material properties [33]

No.	Property	Symbol [Unit]	Value
1	Seebeck coefficient	$S$ [V/K]	$2.1727 \cdot 10^{-4}$
2	Thermal conductivity	$k$ [W/(m·K)]	1.5678
3	Electrical conductivity	$\sigma$ [S/m]	78934
4	Density	$\rho$ [kg/m <sup>3</sup> ]	7700
5	Heat capacity	$C_p$ [J/(kg·K)]	154

## CREDIT AUTHORSHIP CONTRIBUTION

- C. Săvescu: conceptualization, formal analysis, investigation (numerical simulations, experiment), methodology, data curation, validation, visualization, writing (draft, review, and editing).  
 A. Morega: conceptualization, investigation, validation, supervision.  
 M. Roman: investigation (experiment), writing (draft), methodology.  
 C. Nechifor: formal analysis, investigation (measuring), software (DAQ).

Received on 16 April 2025

## REFERENCES

- D. Dima, A. Dobrovicescu, C. Ioniță, C. Dobre, *Exergy analysis of the coupling of two CO<sub>2</sub> heat pump cycles*, Rev. Roum. Sci. Techn. – Électrotechn. et Énerg., **68**, 2, pp. 236–240 (2023).
- A. Mitru, *Data communication and software development for the automation of an industrial piston compressor*, Rev. Roum. Sci. Techn. – Électrotechn. et Énerg., **70**, 1, pp. 97–102 (2025).
- T. Stănescu, D. Ușeriu, *Performance analysis of curved shape on the inlet guide vanes in centrifugal blowers*, Aerosp. Res. Bulg., **36**, pp. 147–156 (2024).
- D. Talah, H. Bentarzi, G. Mangola, *Modeling and simulation of an operating gas turbine using Modelica language*, Rev. Roum. Sci. Techn. – Électrotechn. et Énerg., **68**, 1, pp. 102–107 (2023).
- F. Niculescu, A. Săvescu, A. Mitru, *Transmitting data over the network using an OPC server*, MATEC Web of Conferences, **210**, p. 03002 (2018).
- S. Priya, D. J. Inman, Eds., *Energy Harvesting Technologies*, Boston, MA: Springer US (2009).
- K. U. Laszczyk, P. Śliwiński, K. Kobashi, *Chapter 7 – Energy Harvesting*, Microsupercapacitors, K. Kobashi, K. Laszczyk, Eds. Woodhead Publishing, pp. 205–212 (2022).
- R. Dauksevičius, D. Briand, *Energy Harvesting*, in Material-Integrated Intelligent Systems - Technology and Applications, John Wiley & Sons, Ltd, pp. 479–528 (2018).
- N. Bizon, N. Mahdavi Tabatabaei, F. Blaabjerg, E. Kurt, Eds., *Energy harvesting and energy efficiency: technology, methods, and applications*, **37**. Cham: Springer International Publishing (2017).
- L. Dhakar, *Overview of energy harvesting technologies*, Triboelectric Devices for Power Generation and Self-Powered Sensing Applications, L. Dhakar, Ed. Singapore: Springer, pp. 9–37 (2017).
- S. W. Yufenyuy, G. M. Mengata, L. Nneme Nneme, U. M. Bongwirnso, *Indoor environment PV applications: estimation of the maximum harvestable power*, Renew. Sustain. Energy Rev., **193**, p. 114287 (2024).
- R. Maity, M. Khairul, K. Sudhakar, A. Razak, *Forestvoltaics, floatovoltaics and building applied photovoltaics (BAPV) potential for a university campus*, Energ. Eng., **121**, 9, pp. 2331–2361 (2024).
- D. D’Agostino, F. Minelli, M. D’Urso, F. Minichiello, *Fixed and tracking PV systems for net zero energy buildings: comparison between yearly and monthly energy balance*, Renew. Energy, **195**, pp. 809–824 (2022).
- R. Duirasamy, V. Thiyagarajan, *A novel fault-tolerant generalized symmetrical topology for renewable energy and electric vehicle applications*, Rev. Roum. Sci. Techn. – Électrotechn. et Énerg., **69**, 4, pp. 383–388 (2024).
- M. A. Shoaib, M. F. Khan, B. Ali, *Experimental study to gauge the influence of tilt angle on photovoltaic panel performance*, Rev. Roum. Sci. Techn. – Électrotechn. et Énerg., **70**, 1, pp. 139–144 (2025).
- R. Rai, M. Ishak, S. Kumarasamy, A. Bin Mohd Halil, M. M. Quazi, *Laser treated super hydrophobic glass for solar PV self cleaning application: a SWOT-TWOS-based analysis*, Mater. Res. Express, **12**, 1, p. 012003 (2025).
- B. Safaei, S. Erdem, M. Karimzadeh Kolamroudi, S. Arman, *State-of-the-art review of energy harvesting applications by using thermoelectric generators*, Mech. Adv. Mater. Struct., **31**, 22, pp. 5605–5637 (2024).
- A. Prasad, R. C. Thiagarajan, *Multiphysics modeling and development of thermoelectric generator for waste heat recovery*, COMSOL Conference 2018, Bangalore, India, 9 August 2018.
- G. Pennelli, E. Dimaggio, M. Macucci, *Electrical and thermal optimization of energy-conversion systems based on thermoelectric generators*, Energy, **240**, p. 122494 (2022).
- Z. Varga, E. Rácz, *Experimental investigation of the performance of a thermoelectric generator*, 2022 IEEE 20th Jubilee World Symposium on Applied Machine Intelligence and Informatics (SAMII), pp. 159–164, March 2022.
- S. Singh, R. K. Maurya, S. K. Pandey, *Investigation of thermoelectric properties of ZnV<sub>2</sub>O<sub>4</sub> compound at high temperatures*, J. Phys. D: Appl. Phys., **49**, 42, p. 425601 (2016).
- M. Nesarajah, G. Frey, *Multiphysics simulation in the development of thermoelectric energy harvesting systems*, J. Electron. Mater., **45**, 3, pp. 1408–1411 (2016).
- A. Belkaid, I. Colak, K. Kayisli, *A direct adaptive sliding mode high voltage gain peak power tracker for thermoelectric applications*, Rev. Roum. Sci. Techn. – Électrotechn. et Énerg., **66**, 2, pp. 131–136 (2021).
- \*\*\*TE-MOD-10W4V-40, www.tegpro.com (2014), <https://www.tegmart.com/datasheets/TGPR-10W4V-40S.pdf>.
- \*\*\*COMSOL Multiphysics Reference Manual (2023), [https://doc.comsol.com/6.2/doc/com.comsol.help.comsol/COMSOL\\_ReferenceManual.pdf](https://doc.comsol.com/6.2/doc/com.comsol.help.comsol/COMSOL_ReferenceManual.pdf).
- C. Săvescu, A. Morega, Y. Veli, V. Petrescu, *Numerical modelling of thermoelectric energy harvesting from industrial compressor waste heat*, 13th International Symposium on Advanced Topics in Electrical Engineering (ATEE), Bucharest, Romania, 23 March 2023.
- M. Roman, C. Săvescu, A. Săvescu, R. Stoica, D. Comeaga, *Thermoelectric generator simulations with and without heatsink*, Iberian COMSOL Multiphysics Conference 2024, Málaga, Spain, 28 June 2024.
- C. Săvescu, V. Petrescu, D. Comeaga, R. Carlanescu, M. Roman, D. Lale, A. Mitru, *Thermal potential of a twin-screw compressor as thermoelectric energy harvesting source*, Eng. Technol. Appl. Sci. Res., **14**, 2, pp. 13449–13455 (2024).
- C. Borzea, V. Petrescu, I. Vlăduță, M. Roman, G. Badea, *Potential of twin-screw compressor as vibration source for energy harvesting applications*, APME, **17**, 1, pp. 91–96 (2021).
- C. Borzea (Săvescu), *Multisource Piezoelectric and Thermoelectric Energy Harvesting System for Industrial Machinery*, Doctorate Thesis, National University of Science and Technology Politehnica Bucharest, Bucharest, Romania (2024).
- C. Săvescu, D. Comeagă, M. Roman, D. Lale, R. Stoica, E. Vasile, C. Nechifor, A. Stoicescu, *Experimental study of a piezoelectric harvester vibrating on an industrial screw compressor*, Rev. Roum. Sci. Techn. – Électrotechn. et Énerg., **70**, 1, pp. 9–14 (2025).
- J. Dongxu, W. Zhongbao, J. Pou, S. Mazzoni, S. Rajoo, A. Romagnoli, *Geometry optimization of thermoelectric modules: Simulation and experimental study*, Energy Convers. Manag., **195**, pp. 236–243 (2019).
- \*\*\*Thermoelectric Cooler Design App, COMSOL (2023), <https://www.comsol.com/model/thermoelectric-cooler-30611>.
- G. M. Guttman, Y. Gelbstein, *Mechanical Properties of Thermoelectric Materials for Practical Applications*, in Bringing Thermoelectricity into Reality, IntechOpen (2018).
- \*\*\*Module Installation Notes, www.tegpro.com, <https://www.tegmart.com/datasheets/TGPR-MOD-INST.pdf>.
- \*\*\*TE-MOD-10W4V-40 Datasheet rev. 1.0, Tegmart.com (2014), <https://www.tegmart.com/datasheets/TGPR-10W4V-40S.pdf>.